

# Exact solution of a linear molecular motor model driven by two-step fluctuations and subject to protein friction

Hans C. Fogedby\*

*Institute of Physics and Astronomy, University of Aarhus, DK-8000, Aarhus C, Denmark  
and NORDITA, Blegdamsvej 17, DK-2100, Copenhagen Ø, Denmark*

Ralf Metzler†

*NORDITA, Blegdamsvej 17, DK-2100, Copenhagen Ø, Denmark*

Axel Svane‡

*Institute of Physics and Astronomy, University of Aarhus, DK-8000, Aarhus C, Denmark*

(Received 18 December 2003; published 16 August 2004)

We investigate by analytical means the stochastic equations of motion of a linear molecular motor model based on the concept of protein friction. Solving the coupled Langevin equations originally proposed by Mogilner *et al.* [Phys. Lett. A **237**, 297 (1998)], and averaging over both the two-step internal conformational fluctuations and the thermal noise, we present explicit, analytical expressions for the average motion and the velocity-force relationship. Our results allow for a direct interpretation of details of this motor model which are not readily accessible from numerical solutions. In particular, we find that the model is able to predict physiologically reasonable values for the load-free motor velocity and the motor mobility.

DOI: 10.1103/PhysRevE.70.021905

PACS number(s): 87.16.Nn, 02.50.-r, 05.40.-a, 87.10.+e

## I. INTRODUCTION

There is currently widespread interest in molecular motors, from both a biochemical-physiological and a physics point of view. Whereas the former is mostly concerned with the molecular structure of motors and their structural interplay with the support on which they move, physicists study the nonequilibrium transport properties of motors and their physical interactions with the support, such as load-velocity relations or adhesion forces between motor and support. Molecular motors, in general, are energy consuming, nonequilibrium nanoscale engines, which are encountered in various dynamical processes on the intra- and intercellular level [1–3]; for a recent review of the more physical aspects see, for instance, Ref. [4]. Such motors are responsible for intracellular transport of molecules and small vesicles in eukaryotic cells; they are powering genomic transcription and translation, cell division (mitosis), and the packaging of viral DNA into nanoscale transport containers (capsids) [5–10]. Larger assemblies of motors working in unison are responsible for the motility of, e.g., bacteria, they play a role in cell growth, and they are responsible for muscle contraction leading to macroscopic motion [1,2,4,11].

Linear motor proteins like myosin, kinesin, dynein, DNA helicase, or RNA polymerase are driven by the cyclical hydrolysis of ATP into ADP and inorganic phosphate and wander along linear, polar biomolecular tracks such as actin filaments, microtubules, RNA, or DNA. The motion is typically associated with two- or multistep conformational changes in

the motor protein in interaction with ATP and the filament support, and takes place in a thermal environment subject to viscous forces.

Modern experimental techniques in biology and biophysics, in particular single biomolecule manipulation by, for example, optical tweezers or microneedles, and single particle tracking methods, have yielded considerable insight into the mechanism and the relevant physical scales in molecular motor behavior [12–19]. The typical size of a molecular motor is of order 10–20 nm, moving with a step size of order 8 nm, e.g., kinesin on microtubules, with one ATP molecule hydrolyzed on the average per step. The velocities of molecular motors range from nm/s to  $\mu\text{m/s}$  and the maximum load is of the order of several piconewtons (e.g.,  $\sim 6$  pN for kinesin on microtubules). However, the latter can reach up to 57 pN for the rotating packaging motor of bacteriophages [20]. The time scale of the chemical cycle is a few milliseconds and the average energy input from the ATP-ADP cycle is of order 15–20  $kT$ .

A biomolecular motor represents an interesting and ubiquitous nonequilibrium system operating in the classical regime and is thus directly amenable to an analysis using standard methods within nonequilibrium statistical physics. Physical modeling of molecular motors has thus been studied intensively in recent years both from the point of view of the fundamental underlying physical principles and with regard to specific modeling of concrete motors [9,21–31]. More recently, the concerted action of multiple motors has been considered, such as the action of elastically [32] and rigidly [11] coupled motors, for instance, in muscles [33]. Motors interacting with freely polymerizing microtubules or actin filaments give rise to rich pattern formation such as asters [34], and are responsible for the formation of the contractile ring emerging during cell division [35,36].

\*Electronic address: fogedby@phys.au.dk

†Electronic address: metz@nordita.dk

‡Electronic address: svane@phys.au.dk

The most common statistical approach to molecular motors is that of a ratchet model [4,25], mimicking the periodically alternating energy landscape (given by the interaction potential with its support) perceived by the motor during its mechanochemical cycle. Such ratchet models date back to Smoluchowski [37] and Feynman [38], and Huxley's pioneering work [39] on motor proteins actually corresponds to a Brownian ratchet [4]. We note that ratchets play a much more general role, and real-space ratchets may even be used on the microscale for particle separation [40–42].

An alternative motor model can be based on protein friction [22,25,43–46]. This concept relies on the idea that, due to the weak chemical bonds forming between motor protein and the polar actin or microtubule track, after elimination of the detailed degrees of freedom, an effective friction  $\zeta_p$  builds up between motor and track. This protein friction  $\zeta_p$  acts like a linear friction if the associated time scale of motion is longer than the characteristic time of the kinetics of motor-track bonds. If not, no protein friction can build up, and the motor is subject only to the smaller viscous drag  $\zeta_v$  due to the environment. The protein friction is therefore highly nonlinear. On the basis of this scenario, Mogilner *et al.* [47] recently studied a simple two-step linear molecular motor represented by two coupled overdamped oscillators driven by a two-step Markov process alternating between a relaxed and a strained state of the oscillators and embedded in a thermal environment represented by additive white noise. The two subprocesses are associated with internal conformational changes of the motor protein such that one subprocess is slow, allowing protein friction to be established, while the other is fast and subject only to solvent friction. By means of a numerical analysis, Mogilner *et al.* show that the system acts like a motor and can carry a load. However, unlike the ratchet models, which operate with an attachment to a periodic polar protein filament, the model of Mogilner *et al.* needs only a “passive” groove in order to perform directed motion, and the “ratcheting” comes about by assuming the asymmetric internal velocity fluctuations, which are then rectified by protein friction. In that sense, it is a robotic model of molecular motors.

In the present paper we reanalyze the motor model of Mogilner *et al.* from a purely analytical point of view and derive explicit expressions for the motion of the motor and the velocity-load relationship. Using the biological parameter values quoted by Mogilner *et al.* we show that the model gives rise to physiologically reasonable values for the motor velocity, whereas our analysis leads to a correction of the maximum load force by an order of magnitude in comparison with the numerical results obtained in Ref. [47]. This discrepancy is associated with a difference in the dynamics of the analytical model as compared with the numerical simulation. Allowing for a larger relaxation rate the analytical result for the maximum load force approaches the biological regime. The paper is organized in the following manner. In Sec. II we introduce the model. In Sec. III we solve the model analytically. In Sec. IV we discuss the results and compare with Ref. [47]. The paper ends with a summary and a conclusion in Sec. V.

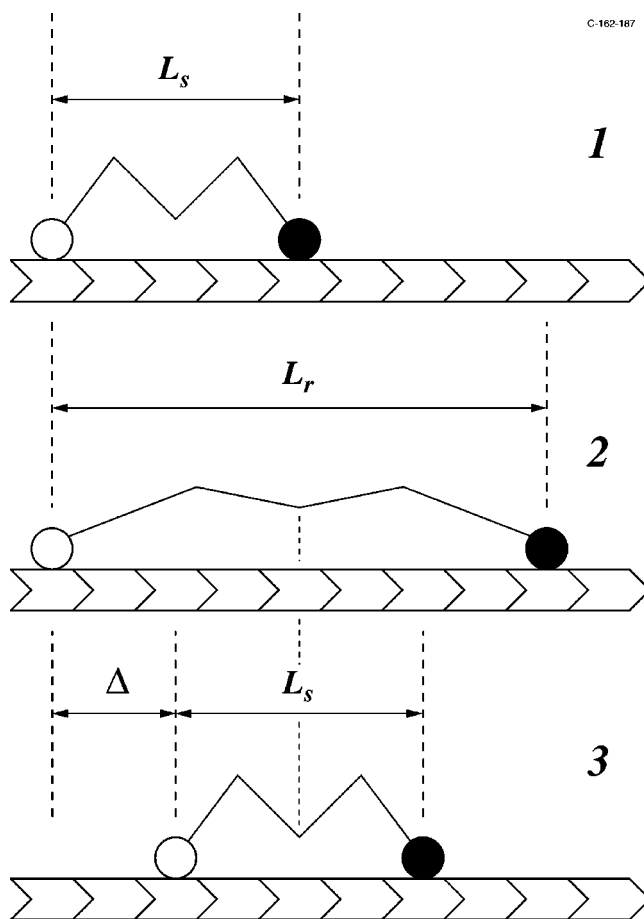


FIG. 1. Molecular motor model showing one mechanochemical cycle, during which internal fluctuations become directed (“ratcheted”) through protein friction. The conformational changes of the motor protein are represented by two states of an effective spring with rest lengths  $L_s$  for the strained and  $L_r$  for the relaxed states. 1  $\rightarrow$  2: Slow relaxation of the previously strained spring to assume the rest length  $L_r$ ; due to protein friction, the white working head of the motor stays attached to the polar biopolymer (actin filament or microtubule), while the black idle head is free to move. 2  $\rightarrow$  3: As a consequence of ATP hydrolysis (“power stroke”), the spring contracts so quickly that the protein friction breaks down, and both heads symmetrically converge to assume the strained configuration with rest length  $L_s$ . The distance covered per mechanochemical cycle is  $\Delta = (L_r - L_s)/2$ . (Adapted from Ref. [47].)

## II. MODEL

The motor model based on protein friction which was introduced in Ref. [47] is defined as follows (compare Fig. 1). Assume that the mechanochemical cycle of the motor protein moving along a track made up of an actin filament or microtubule can be pinned down to the periodical switching between two states, and that each of these two states can be described by two motor heads connected by an effective spring representing the backbone of the motor protein between these heads. From the strained state ( $S$ ), characterized by a rest length  $L_s$ , the motor protein converges toward a relaxed state ( $R$ ) with rest length  $L_r > L_s$ , i.e., the distance between the motor heads increases. This process is slow

enough to make sure that the adhesion between the motor's "working head" (white circle in Fig. 1) and track stays intact, in such a manner that asymmetric motion with respect to the track is achieved (stick). In contrast, during the fast "power stroke" from the relaxed state back to the strained state after hydrolysis of ATP, the protein friction is broken and both heads move under the low Reynolds number conditions of the environment, such that both heads symmetrically approach each other and assume the rest length  $L_s$  (slip).

This model can be cast into the two coupled Langevin equations

$$\zeta(t)\dot{x}(t) = -f + k(t)\frac{y(t) - x(t) - L(t)}{2} + N_x(t), \quad (2.1)$$

$$\zeta_v\dot{y}(t) = -k(t)\frac{y(t) - x(t) - L(t)}{2} + N_y(t), \quad (2.2)$$

in which we have introduced the time-dependent friction coefficient  $\zeta(t)$  in comparison to Ref. [47] for convenience, to account for the cyclical attachment to the track. In Eqs. (2.1) and (2.2) the variables  $x$  and  $y$  represent the positions of the two heads of the motor molecule along the track, corresponding to the equations of motion of two coupled, overdamped oscillators. The coordinate of the idle head  $y$  is associated with a viscous friction drag coefficient  $\zeta_v$  of order  $6\pi\eta r$  (Stokes law), where  $\eta$  is the viscosity of water and  $r$  the size of the motor protein head. The same friction acts on the working head during the fast conformational change  $R \rightarrow S$ , whereas during the slow process  $S \rightarrow R$ , it experiences the protein friction drag with coefficient  $\zeta_p$  [22,25,43–46], corresponding to a stick-slip motion of the working head. The model equations (2.1) and (2.2) are driven by thermal noises  $N_x(t)$  and  $N_y(t)$ , with  $\langle N_{x,y}(t) \rangle = 0$ , representing the ambient environment with correlations

$$\langle N_{x,y}(t)N_{x,y}(t') \rangle = 2k_B T \zeta_{p,v} \delta(t - t'), \quad (2.3)$$

balancing the friction terms by means of the fluctuation-dissipation theorem. We note that during the detached straining step, the role of working and idle heads may be exchanged (i.e., the motor heads may be turned around a common axis), as was recently demonstrated for kinesin motor heads [48].

The conformational changes of the motor driven by the ATP-ADP hydrolytic cycle and the cyclical attachment to the substrate correspond to a continuous two-state Markov process for the time-dependent rest length  $L(t)$ , the time-dependent spring constant  $k(t)$ , and the time-dependent protein friction  $\zeta(t)$ , alternating between state  $R$  with rest length  $L_r$ , spring constant  $k_r$ , and protein friction  $\zeta = \zeta_p$  and state  $S$  with rest length  $L_s$ , spring constant  $k_s$ , and viscous friction  $\zeta = \zeta_v$ . The power stroke conformational transition  $R \rightarrow S$  driven by the ATP hydrolysis is characterized by the rate  $g_s$ ; the relaxational conformation change  $S \rightarrow R$  has the rate  $g_r$ .

The relevant biological parameters quoted in Ref. [47], entering Eqs. (2.1) and (2.2), are the rate of hydrolysis  $g_s \sim 10^3 \text{ s}^{-1}$ , the relaxation rate  $g_r \sim 10^3 \text{ s}^{-1}$ , the spring coefficient in the relaxed state  $k_r \sim 0.01 \text{ pN/nm}$ , the spring coefficient in the strained state  $k_s \sim 0.5 \text{ pN/nm}$ , the rest length in

the relaxed state  $L_r \sim 40 \text{ nm}$ , the rest length in the strained state  $L_s \sim 20 \text{ nm}$ , the viscous drag coefficient  $\zeta_v \sim 10^{-6} \text{ pN s/nm}$ , the protein friction drag coefficient  $\zeta_p \sim 5 \times 10^{-5} \text{ pN s/nm}$ , and the load force  $f \sim \pm 1 \text{ pN}$ . For further discussion of the model and parameter choices under biological conditions we refer to Ref. [47]. An important difference between the model of Mogilner *et al.* and the present one in Eqs. (2.1) and (2.2) is that we take  $\zeta(t) = \zeta_v$  during the entire duration of the strained state  $S$ , while Mogilner assumes  $\zeta(t) = \zeta_v$  only in the first short time interval as the spring contracts (a time interval of order  $t_{\text{slip}} \sim \zeta_v/k_s$ ; in the simulations of Ref. [47]  $t_{\text{slip}}$  is taken infinitesimally small), after which the protein bonds will form and protein friction take over,  $\zeta(t) = \zeta_p$ . The two models will be similar if the relaxation time  $g_r^{-1}$  is of the order of  $t_{\text{slip}}$ .

### III. ANALYSIS

In this section, we present a solution scheme for this motor model. The results obtained are then further analyzed in the following section.

#### A. Analytical solution

The motor equations (2.1) and (2.2) are readily analyzed by (i) solving Eq. (2.1) for  $y(t)$  and deriving  $dy/dt$ , and (ii) eliminating  $y$  in Eq. (2.2) and setting the two expressions equal to one another. We thus obtain the following equations for  $v_x = dx/dt$  and  $v_y = dy/dt$ :

$$\begin{aligned} 2(\zeta\zeta_v/k)\dot{v}_x + [\zeta + \zeta_v - 2\zeta\zeta_v(\dot{k}/k^2) + 2\dot{\zeta}\zeta_v/k]v_x \\ = -f(1 - 2\zeta_v(\dot{k}/k^2)) - \zeta_v\dot{L} + 2\zeta_v\dot{N}_x/k \\ + (1 - 2\zeta_v\dot{k}/k^2)N_x + N_y, \end{aligned} \quad (3.1)$$

$$\zeta_v v_y = -f - \zeta v_x + N_x + N_y. \quad (3.2)$$

Denoting the initial velocity at time  $t=0$  by  $v_{x0}$  Eq. (3.1) is readily solved by quadrature and together with Eq. (3.2) we obtain

$$\begin{aligned} v_x(t) = \frac{k(t)e^{-\gamma(t)}}{\zeta(t)} \left[ v_{x0} \frac{\zeta(0)}{k(0)} - \frac{1}{2\zeta_v} \int_0^t dt' \right. \\ \left. \times [\tilde{f}(t') + \zeta_v \dot{L}(t') - \tilde{N}(t')] e^{\gamma(t')} \right], \end{aligned} \quad (3.3)$$

$$v_y(t) = -\frac{f}{\zeta_v} - \frac{\zeta(t)}{\zeta_v} v_x(t) + \frac{1}{\zeta_v} [N_x(t) + N_y(t)] \quad (3.4)$$

which form the basis for our discussion.

We have introduced the renormalized load force  $\tilde{f}$ , the renormalized noise  $\tilde{N}$ , and the integrated spring and friction constant  $\gamma$ :

$$\tilde{f} = f(1 - 2\zeta_v(\dot{k}/k^2)), \quad (3.5)$$

$$\tilde{N} = 2\zeta_v\dot{N}_x/k + (1 - 2\zeta_v\dot{k}/k^2)N_x + N_y, \quad (3.6)$$

$$\gamma(t) = (1/2\zeta_v) \int_0^t k(t') dt' + \int_0^t k(t')/2\zeta(t') dt'. \quad (3.7)$$

### B. General properties

We note various general features of this solution. First, both the load force  $f$  and the thermal noises  $N_x$  and  $N_y$  are renormalized by the fluctuating spring constant  $k$ . Second, the thermal noise basically enters additively and entails thermal fluctuations of the velocities. Since the stochastic conformational changes giving rise to the fluctuations of  $k$ ,  $L$ , and  $\zeta$  are independent of the thermal fluctuations we can, in order to monitor the time dependence of the mean motor velocity, average over the noise with impunity. Note that the heat bath, of course, still enters through the friction coefficients. In the long time steady state limit we can ignore the initial terms and obtain the reduced equations for the thermally averaged velocities

$$v_x(t) = - \frac{k(t)e^{-\gamma(t)}}{2\zeta_v\zeta(t)} \int_0^t dt' [\tilde{f}(t') + \zeta_v \dot{L}(t')] e^{\gamma(t')}, \quad (3.8)$$

$$v_y(t) = + \frac{k(t)e^{-\gamma(t)}}{2\zeta_v^2} \int_0^t dt' [\tilde{f}(t') + \zeta_v \dot{L}(t')] e^{\gamma(t')} - \frac{f}{\zeta_v}, \quad (3.9)$$

which we proceed to discuss.

### C. Constant spring constant and rest length

Let us first consider as an illustration the case of a constant spring length  $L$ , a constant spring constant  $k$ , and a constant protein friction  $\zeta(t) = \zeta_p$ . In this simple case  $\gamma(t) = k[(\zeta_p + \zeta_v)/2\zeta_p\zeta_v]t$  and the load force is unrenormalized. We obtain

$$v_x = v_y = - \frac{f}{\zeta_p + \zeta_v}. \quad (3.10)$$

Here the load  $f$  after a transient period drives the idle and working heads with a constant mean velocity. Defining the mobility according to

$$v_x = -\mu f, \quad (3.11)$$

we infer the mobility in the absence of conformational fluctuations

$$\mu = \frac{1}{\zeta_p + \zeta_v}. \quad (3.12)$$

In the absence of a load for  $f=0$ , the mean velocity vanishes and the system does not move, i.e., we do not have motor properties. This is also a statement of the second law of thermodynamics expressing the fact that we cannot extract work from a system in thermal equilibrium. In the case of constant  $k$ , constant  $L$ , and constant  $\zeta$  the coupled Langevin equations describe the temporal fluctuations of a system in thermal equilibrium. The motor property is thus necessarily

due to the fluctuating spring constant  $k(t)$  and fluctuating length  $L(t)$  characterizing the conformational fluctuations in combination with the cyclical attachment described by the fluctuating friction coefficient  $\zeta(t)$ .

### D. Fluctuating spring constant, rest length, and protein friction

The idea behind the model is that fluctuations of the spring constant  $k(t) = k_s, k_r$  ( $k_r < k_s$ ) and rest length  $L(t) = L_s, L_r$  ( $L_r > L_s$ ), modeling the ATD-ADP driven conformational changes, provide an energy source. In combination with the synchronized stick-slip mechanism modeled by a fluctuating protein friction  $\zeta(t) = \zeta_p, \zeta_v$  ( $\zeta_p > \zeta_v$ ), this process can drive the system in the absence of a force. This mechanism is modeled by the two-step Markovian process  $S \leftrightarrow R$  with relaxation rates  $g_r$  for  $S \rightarrow R$  and  $g_s$  for  $R \rightarrow S$ . The master equations for this process denoting the corresponding probabilities by  $P_s(t)$  and  $P_r(t)$  thus take the form

$$\frac{dP_s(t)}{dt} = g_s P_r(t) - g_r P_s(t), \quad (3.13)$$

$$\frac{dP_r(t)}{dt} = g_r P_s(t) - g_s P_r(t), \quad (3.14)$$

with stationary solutions

$$P_s = \frac{g_s}{g_s + g_r}, \quad (3.15)$$

$$P_r = \frac{g_r}{g_s + g_r}. \quad (3.16)$$

The stationary mean value of, e.g., the spring constant, is thus given by

$$k_{st} = k_s P_s + k_r P_r = \frac{k_s g_s + k_r g_r}{g_s + g_r}. \quad (3.17)$$

For the present purposes it turns out to be more convenient in discussing the conformational transitions to focus on the probability distributions  $\tilde{P}_s(t)$  and  $\tilde{P}_r(t)$  characterizing the residence of the system in either the strained state or the relaxed state at a time  $t$ . The distribution is exponential in time and we obtain properly normalized

$$\tilde{P}_s(t) = g_r e^{-g_r t}, \quad (3.18)$$

$$\tilde{P}_r(t) = g_s e^{-g_s t}. \quad (3.19)$$

The mean values of the residence times are then given by

$$\langle t \rangle_s = \frac{1}{g_r}, \quad (3.20)$$

$$\langle t \rangle_r = \frac{1}{g_s}. \quad (3.21)$$

The mean value of  $k$  may then be obtained as a time average:

$$\langle k \rangle = \frac{k_s \langle t \rangle_s + k_r \langle t \rangle_r}{\langle t \rangle_s + \langle t \rangle_r} = \frac{k_s/g_r + k_r/g_s}{1/g_r + 1/g_s}, \quad (3.22)$$

in accordance with Eq. (3.17).

### E. The motor property without a load

Here we establish the fundamental motor property of the model in the absence of a load. For  $f=0$  we have from Eqs. (3.8) and (3.9)

$$v_x^0 = -\frac{k(t)e^{-\gamma(t)}}{2\zeta(t)} \int_0^t dt' \dot{L}(t') e^{\gamma(t')}, \quad (3.23)$$

$$v_y^0 = +\frac{k(t)e^{-\gamma(t)}}{2\zeta_v} \int_0^t dt' \dot{L}(t') e^{\gamma(t')}, \quad (3.24)$$

At a superficial glance it looks as if the motor heads move in opposite directions. However, subtracting the velocities and noting that

$$\dot{\gamma}(t) = \frac{k(t)}{2\zeta(t)} + \frac{k(t)}{2\zeta_v}, \quad (3.25)$$

we obtain

$$v_x^0 - v_y^0 = -\dot{\gamma}(t) e^{-\gamma(t)} \int_0^t dt' \dot{L}(t') e^{\gamma(t')}. \quad (3.26)$$

Finally, assuming ergodicity (to be established later) and time averaging in combination with partial integrations we have for  $T \rightarrow \infty$

$$\begin{aligned} \langle v_x^0 \rangle - \langle v_y^0 \rangle &= -\frac{1}{T} \int_0^T dt \dot{\gamma}(t) e^{-\gamma(t)} \int_0^t dt' \dot{L}(t') e^{\gamma(t')} \\ &= \frac{1}{T} \int_0^T dt \frac{d}{dt} [e^{-\gamma(t)}] \int_0^t dt' \dot{L}(t') e^{\gamma(t')} \\ &= -\frac{1}{T} \int_0^T \dot{L}(t) dt = 0, \end{aligned} \quad (3.27)$$

where the last step corresponds to an integration by parts (note that  $\gamma(t)$  is monotonically increasing, and therefore  $T^{-1}[\int_0^T \dot{L}(t') \exp\{\gamma(t') - \gamma(t)\}]_0^T < T^{-1}[L(t)]_0^T \rightarrow 0$ ), and we conclude that the average velocities of the two heads are in fact identical: The working head and the idle head move together.

Next we derive an explicit expression for  $\langle v_x^0 \rangle$ . Introducing the auxiliary fluctuating variable

$$a(t) = \frac{k(t)}{2} \left[ \frac{1}{\zeta_v} - \frac{1}{\zeta(t)} \right], \quad (3.28)$$

and using the above result we obtain by adding Eqs. (3.23) and (3.24):

$$\langle v_x^0 \rangle = \frac{1}{2} \int_0^t dt' \langle e^{-[\gamma(t) - \gamma(t')]} a(t) \dot{L}(t') \rangle. \quad (3.29)$$

Here  $\langle \dots \rangle$  denotes an ensemble average with respect to the conformational fluctuations. Since  $L(t)$ ,  $k(t)$ , and  $\zeta(t)$  are

governed by the same stochastic process, with the values  $L_s$ ,  $\zeta_v$ ,  $k_s$ , and  $L_r$ ,  $\zeta_p$ ,  $k_r$  in the strained and relaxed states, respectively, we obtain from the expressions for  $a$  and  $\dot{\gamma}$  in Eqs. (3.28) and (3.7)

$$a_r = \frac{k_r}{2} \left[ \frac{1}{\zeta_v} - \frac{1}{\zeta_p} \right], \quad (3.30)$$

$$a_s = 0, \quad (3.31)$$

$$\dot{\gamma}_r = \frac{k_r}{2} \left[ \frac{1}{\zeta_v} + \frac{1}{\zeta_p} \right], \quad (3.32)$$

$$\dot{\gamma}_s = \frac{k_s}{\zeta_v}. \quad (3.33)$$

Denoting the jump times for the transitions between the strained and relaxed state by  $t_n$ ,  $n=1, 2, \dots$ , and assuming that the system is in a relaxed state at  $0 < t < t_1$  we have

$$\dot{L}(t) = (L_r - L_s) \sum_{n=1}^{\infty} (-1)^n \delta(t - t_n), \quad (3.34)$$

and inserting this in Eq. (3.29) we obtain

$$\langle v_x^0 \rangle = \frac{L_r - L_s}{2} \sum_{n=1}^N (-1)^n \left\langle a(t) \exp\left(-\int_{t_n}^t \dot{\gamma}(t') dt'\right) \right\rangle, \quad (3.35)$$

where  $t_N < t < t_{N+1}$ . Note that the exponential term is just a more complicated way to write  $\exp\{-\gamma(t) + \gamma(t_n)\}$ , which will be useful below. For even  $N$  the system is in the relaxed state for  $t_N < t' < t$  with probability  $P_r$ . Similarly, for odd  $N$  the motor ends in the strained state which occurs with probability  $P_s$ . Introducing the time interval  $\tau_n = t_{n+1} - t_n$ , noting that the residence distributions are statistically independent, and introducing the notation

$$R = \langle \exp(-\dot{\gamma}_r \tau) \rangle_r = \int_0^{\infty} d\tau \tilde{P}_r(\tau) \exp(-\dot{\gamma}_r \tau) = \frac{g_s}{g_s + \dot{\gamma}_r}, \quad (3.36)$$

$$S = \langle \exp(-\dot{\gamma}_s \tau) \rangle_s = \int_0^{\infty} d\tau \tilde{P}_s(\tau) \exp(-\dot{\gamma}_s \tau) = \frac{g_r}{g_r + \dot{\gamma}_s}, \quad (3.37)$$

the mean velocity can be expressed in terms of geometrical series,

$$\begin{aligned} \langle v_x^0 \rangle &= \frac{L_r - L_s}{2} \left[ P_r a_r R (1 - S) \sum_{n=0}^{\infty} (SR)^n \right. \\ &\quad \left. - P_s a_s S (1 - R) \sum_{n=0}^{\infty} (SR)^n \right], \end{aligned} \quad (3.38)$$

or, summing the series (completing  $N \rightarrow \infty$ ),

$$\langle v_x^0 \rangle = \frac{L_r - L_s P_r a_r R(1-S) - P_s a_s S(1-R)}{2(1-RS)}. \quad (3.39)$$

Inserting  $P_r$ ,  $P_s$ ,  $R$ , and  $S$  from Eqs. (3.15), (3.16), (3.36), and (3.37) we arrive at

$$\langle v_x^0 \rangle = \frac{L_r - L_s}{2} \frac{g_r g_s (a_r \dot{\gamma}_s - a_s \dot{\gamma}_r)}{(g_s \dot{\gamma}_s + g_r \dot{\gamma}_r + \dot{\gamma}_r \dot{\gamma}_s)(g_s + g_r)}. \quad (3.40)$$

First we note that the expression vanishes for  $a(t) = \dot{\gamma}(t)$  thus corroborating the validity of the time average in Eq. (3.27) and establishing ergodicity. Finally, inserting  $a_r$ ,  $a_s$ ,  $\dot{\gamma}_r$ , and  $\dot{\gamma}_s$  from Eqs. (3.30)–(3.33), we obtain for the explicit expression for the motor velocity in the absence of a load

$$\langle v_x^0 \rangle = \frac{(L_r - L_s)(\zeta_p - \zeta_v)k_r k_s g_r g_s}{2(g_r + g_s)[2g_s k_s \zeta_p \zeta_v + k_r(\zeta_p + \zeta_v)(g_r \zeta_v + k_s)]}. \quad (3.41)$$

### F. The motor property with load

We next turn to the case of a load force applied to the motor. First we establish that in the presence of the load the two heads of the motor move together with the same average velocity. From Eqs. (3.8) and (3.9) we obtain

$$v_x - v_y = v_x^0 - v_y^0 - \frac{\dot{\gamma}(t)e^{-\gamma(t)}}{\zeta_v} \int_0^t dt' \tilde{f}(t') e^{\gamma(t')} + \frac{f}{\zeta_v}. \quad (3.42)$$

Inserting  $\tilde{f}$  from Eq. (3.5) and averaging over time we have, using Eq. (3.27),

$$\begin{aligned} \langle v_x \rangle - \langle v_y \rangle &= -\frac{f}{\zeta_v} \frac{1}{T} \int_0^T dt e^{-\gamma(t)} \dot{\gamma}(t) \int_0^t dt' e^{\gamma(t')} + \frac{f}{\zeta_v} \\ &\quad + f \frac{2}{T} \int_0^T dt e^{-\gamma(t)} \dot{\gamma}(t) \int_0^t dt' \frac{\dot{k}(t')}{k(t')^2} e^{\gamma(t')}. \end{aligned} \quad (3.43)$$

Performing the integrals by partial integration along the same lines as in the load-free case, the first two terms in Eq. (3.43) cancel, and we find in the limit  $T \rightarrow \infty$ ,

$$\langle v_x \rangle = \langle v_y \rangle, \quad (3.44)$$

i.e., the two motor heads move together with the same average velocity.

We now turn to the evaluation of the load-velocity relationship. From Eqs. (3.8) and (3.9) and inserting  $\tilde{f}$  we have

$$v_x = v_x^0 - \frac{f}{2\zeta_v} \int_0^t dt' \frac{k(t)}{\zeta(t)} \left[ 1 + 2\zeta_v \frac{d}{dt'} \left( \frac{1}{k(t')} \right) \right] e^{-[\gamma(t) - \gamma(t')]}, \quad (3.45)$$

$$v_y = v_y^0 - \frac{f}{\zeta_v} + \frac{f}{2\zeta_v} \int_0^t dt' \frac{k(t)}{\zeta_v} \left[ 1 + 2\zeta_v \frac{d}{dt'} \left( \frac{1}{k(t')} \right) \right] e^{-[\gamma(t) - \gamma(t')]}. \quad (3.46)$$

From the synchronization of the stochastic processes we obtain the identity

$$\frac{1}{k(t)} = \frac{1}{k_r} + \frac{1/k_s - 1/k_r}{\dot{\gamma}_s - \dot{\gamma}_r} [\dot{\gamma}(t) - \dot{\gamma}_r], \quad (3.47)$$

and therefore

$$\frac{d}{dt} \frac{1}{k(t)} = \frac{1/k_s - 1/k_r}{\dot{\gamma}_s - \dot{\gamma}_r} \dot{\gamma}(t). \quad (3.48)$$

Inserting into Eqs. (3.45) and (3.46) and averaging

$$\begin{aligned} \langle v_x \rangle &= \langle v_x^0 \rangle - \frac{f}{2\zeta_v} \left\langle \frac{k(t)}{\zeta(t)} \int_0^t dt' e^{-[\gamma(t) - \gamma(t')]} \right\rangle \\ &\quad - f \frac{1/k_s - 1/k_r}{\dot{\gamma}_s - \dot{\gamma}_r} \left\langle \frac{k(t)}{\zeta(t)} \int_0^t dt' e^{-[\gamma(t) - \gamma(t')]} \dot{\gamma}(t') \right\rangle, \end{aligned} \quad (3.49)$$

$$\begin{aligned} \langle v_y \rangle &= \langle v_y^0 \rangle - \frac{f}{\zeta_v} + \frac{f}{2\zeta_v} \left\langle \frac{k(t)}{\zeta_v} \int_0^t dt' e^{-[\gamma(t) - \gamma(t')]} \right\rangle \\ &\quad + f \frac{1/k_s - 1/k_r}{\dot{\gamma}_s - \dot{\gamma}_r} \left\langle \frac{k(t)}{\zeta_v} \int_0^t dt' e^{-[\gamma(t) - \gamma(t')]} \dot{\gamma}(t') \right\rangle. \end{aligned} \quad (3.50)$$

The first integral in Eqs. (3.49) and (3.50) has the form

$$\begin{aligned} I_1 &= \left\langle b(t) \int_0^t dt' e^{-(\gamma(t) - \gamma(t'))} \right\rangle \\ &= \left\langle b(t) \int_0^t dt \exp\left(-\int_{t'}^t dt'' \dot{\gamma}(t'')\right) \right\rangle, \end{aligned} \quad (3.51)$$

and is performed by breaking up the integration over  $\dot{\gamma}$  in the exponents and averaging over the time segments yielding again a geometrical series in terms of  $SR$ . We obtain as an intermediate result

$$\begin{aligned} I_1 &= P_r b_r \left( \frac{1-R}{\dot{\gamma}_r} + \frac{R(1-S)}{\dot{\gamma}_s} \right) \sum_{n=0} (SR)^n \\ &\quad + P_s b_s \left( \frac{1-S}{\dot{\gamma}_s} + \frac{S(1-R)}{\dot{\gamma}_r} \right) \sum_{n=0} (SR)^n, \end{aligned} \quad (3.52)$$

and performing the sum and inserting  $R$  and  $S$  from Eqs. (3.36) and (3.37),

$$I_1 = \frac{b_r P_r (g_r + g_s + \dot{\gamma}_s) + b_s P_s (g_r + g_s + \dot{\gamma}_r)}{g_s \dot{\gamma}_s + g_r \dot{\gamma}_r + \dot{\gamma}_r \dot{\gamma}_s}. \quad (3.53)$$

The second integral has the structure

$$I_2 = \left\langle c(t) \int_0^t dt' e^{-(\gamma(t)-\gamma(t'))} \dot{\gamma}(t') \right\rangle, \quad (3.54)$$

and was performed in the load-free case in Eqs. (3.35)–(3.40). We found

$$I_2 = - \frac{(\dot{\gamma}_s - \dot{\gamma}_r) P_r P_s (g_s + g_r) (c_r \dot{\gamma}_s - c_s \dot{\gamma}_r)}{g_s \dot{\gamma}_s + g_r \dot{\gamma}_r + \dot{\gamma}_r \dot{\gamma}_s}. \quad (3.55)$$

It is again convenient to introduce the mobility  $\mu$  according to the relation

$$\langle v_x \rangle = \langle v_x^0 \rangle - \mu f, \quad (3.56)$$

and we obtain inserting  $c(t)=b(t)=k(t)/\zeta_p(t)$  for  $\langle v_x \rangle$ , or  $c(t)=b(t)=k(t)/\zeta_v$  for  $\langle v_y \rangle$ ,

$$\mu = + \frac{(k_r/2\zeta_v\zeta_p) P_r (g_r + g_s + \dot{\gamma}_s) + (k_s/2\zeta_v^2) P_s (g_r + g_s + \dot{\gamma}_r)}{g_s \dot{\gamma}_s + g_r \dot{\gamma}_r + \dot{\gamma}_r \dot{\gamma}_s} - \frac{P_r P_s (g_s + g_r) ((k_r/\zeta_p) \dot{\gamma}_s - (k_s/\zeta_v) \dot{\gamma}_r) (1/k_s - 1/k_r)}{g_s \dot{\gamma}_s + g_r \dot{\gamma}_r + \dot{\gamma}_r \dot{\gamma}_s}. \quad (3.57)$$

#### IV. DISCUSSION

In this section, we examine more closely our results derived above, and compare them to the analysis in Ref. [47].

##### A. Free motor

Let us first examine the simple motor properties in the absence of a cargo, i.e., for  $f=0$ . Here the expression in Eq. (3.41) is at variance with the heuristic expression given by Mogilner *et al.* [47],

$$\langle v_x \rangle_M^0 = \frac{g_s g_r}{g_r + g_s} \frac{L_r - L_s}{2}, \quad (4.1)$$

which is solely based on the reaction rates, neglecting the internal dynamics of the motor. To compare the expression

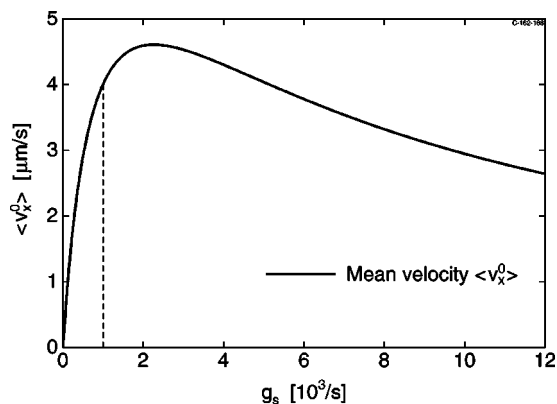


FIG. 2. Dependence of the mean velocity  $\langle v_x^0 \rangle$  on the hydrolysis rate  $g_s$ , exhibiting a maximum at around  $2.25 \times 10^3$ /s. The vertical dashed line shows the parameter value given in Ref. [47]. For large values of  $g_s$ , the velocity tends to zero.

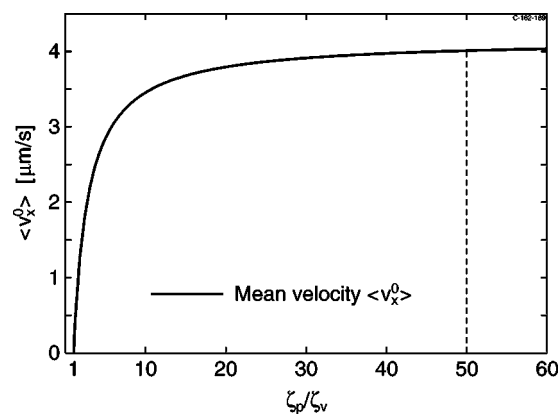


FIG. 3. Dependence of the mean velocity  $\langle v_x^0 \rangle$  on the protein friction  $\zeta_p$ , reaching a plateau for large values ( $\zeta_v = 10^{-6}$  pN s/nm). The protein friction  $\zeta_p = 5 \times 10^{-5}$  nm/s pN used in the calculations corresponds to the dimensionless value 50 in the plot, indicated by the dashed line. Note that  $\langle v_x^0 \rangle = 0$  corresponds to  $\zeta_p/\zeta_v = 1$ .

for the present model, Eq. (3.41), we introduce the dimensionless parameters

$$q_s = \frac{g_r}{\dot{\gamma}_s} \quad (4.2)$$

and

$$q_r = \frac{g_s}{\dot{\gamma}_r}, \quad (4.3)$$

which express the ratio between the spring relaxation times,  $\dot{\gamma}_s^{-1}$  and  $\dot{\gamma}_r^{-1}$ , and the residence times Eqs. (3.20) in states  $S$  and  $R$ , respectively. In terms of these parameters we obtain

$$\langle v_x^0 \rangle = \langle v_x \rangle_M^0 \times \frac{\zeta_p - \zeta_v}{\zeta_p + \zeta_v} \frac{1}{1 + q_s + q_r}. \quad (4.4)$$

The correction factor to the heuristic velocity given by Mogilner *et al.* is clearly smaller than 1, but approaches 1 in the limit of  $\zeta_p \gg \zeta_v$  and  $q_s \ll 1$ ,  $q_r \ll 1$ , which are exactly the conditions under which expression (4.1) was derived.

We note that the velocity vanishes for  $\zeta_p = \zeta_v$ . In this case the attachment to the track has no effect on the friction and there is no motion. In the limit of large protein friction compared to the viscous drag coefficient,  $\zeta_p \gg \zeta_v$ , but  $q_s \sim 1$  and/or  $q_r \sim 1$  each conformational cycle does not yield a full step of length  $\Delta L/2$  due to incomplete spring relaxation, and the average velocity is reduced. In the limit of either  $q_s \gg 1$  or  $q_r \gg 1$  the motor comes to rest, as the relaxation rate or the hydrolysis rate becomes too large for the spring to change its average length. The motor would also function under conditions  $\zeta_v > \zeta_p$  or  $L_s > L_r$ ; it would just move in the opposite direction.

Inserting the characteristic biological numbers from Ref. [47] we have  $\zeta_p/\zeta_v \approx 50$ ,  $q_r \approx 0.2$ , and  $q_s \approx 2 \times 10^{-3}$ , and the correction factor takes a value of about 0.8. This corresponds to a average velocity of  $\langle v_x \rangle^0 \sim 4 \times 10^3$  nm/s. However, under different conditions, the discrepancy between the heuristic result (4.1) and the exact quantity (4.4) may become more significant.

In Figs. 2 and 3, we show the dependence of the load-free velocity on the hydrolysis rate  $g_s$  and the protein friction  $\zeta_p$  (all other parameters fixed at the values of Ref. [47]). Accordingly, with respect to these values the model motor velocity is close to optimum. The maximum in the  $g_s$  dependence shows the interplay between on and off rates in the protein friction model, whereas the final plateau in the  $\zeta_p$  dependence indicates the above-mentioned saturation, i.e., the motor still works for extremely large values of  $\zeta_p$ , as long as  $q_s$  and/or  $q_r$  do not increase to high values as well. We

note that, as expected, the velocity goes to zero for vanishing hydrolysis rate, and when the protein friction approaches  $\zeta_p \rightarrow \zeta_v$ .

## B. Motor carrying a load

In the case of a load or cargo we proceed to discuss the expression for the motor mobility in Eq. (3.57), which can be rewritten in the more convenient form

$$\mu = \frac{2(g_r + g_s)(P_r k_r + P_s k_s)(P_r \zeta_v + P_s \zeta_p) + k_r k_s (1 + P_r + P_s \zeta_p / \zeta_v)}{2\zeta_v \{2g_s k_s \zeta_p + k_r (g_r \zeta_v + k_s)(1 + \zeta_p / \zeta_v)\}}. \quad (4.5)$$

In the further discussion of the mobility it is convenient to introduce the dimensionless parameters in Eqs. (4.2) and (4.3). The expression (4.5) can then be reduced to the form

$$\mu = \frac{(P_r \zeta_v + P_s \zeta_p)[2q_s + (1 + \zeta_v / \zeta_p)q_r] + (1 + P_r)\zeta_v + P_s \zeta_p}{2\zeta_v(\zeta_v + \zeta_p)(1 + q_s + q_r)}. \quad (4.6)$$

Let us investigate this expression in some limiting cases. (i) In the absence of fluctuations, i.e., the case of a constant spring constant and rest length, in the relaxed state  $R$ , the protein friction  $\zeta(t)$  is locked onto  $\zeta_p$ , and we have  $P_r=1$ ,  $P_s=0$  and  $q_r=0$ . By inspection of Eq. (4.6) we then obtain the mobility  $\mu=1/(\zeta_p+\zeta_v)$ , as discussed in Sec. III B. (ii) Similarly, in the strained state  $S$ , the protein friction  $\zeta(t)$  is locked onto  $\zeta_v$ ,  $P_s=1$ ,  $P_r=0$ , and  $q_s=0$ , and we obtain the mobility  $\mu=1/2\zeta_v$ . (iii) Finally, in the case  $\zeta_p=\zeta_v$ , we immediately find  $\mu=1/2\zeta_v$ , as is also evident from the model

equations (2.1) and (2.2). Interpolating between the limiting cases (i) and (ii) above, we introduce the average mobility according to

$$\mu_{\text{av}} = P_r \frac{1}{\zeta_p + \zeta_v} + P_s \frac{1}{2\zeta_v} = \frac{\zeta_v + P_r \zeta_v + P_s \zeta_p}{2\zeta_v(\zeta_p + \zeta_v)}, \quad (4.7)$$

and the mobility in Eq. (4.6) takes the form

$$\mu = \mu_{\text{av}} \frac{1 + \left[2q_s + \left(1 + \frac{\zeta_v}{\zeta_p}\right)q_r\right] \frac{P_r \zeta_v + P_s \zeta_p}{P_r \zeta_v + P_s \zeta_p + \zeta_v}}{1 + q_s + q_r}. \quad (4.8)$$

Inserting the characteristic biological numbers of Mogilner *et al.* [47],  $\zeta_p/\zeta_v=50$ ,  $q_r=0.2$ ,  $q_s=2 \times 10^{-3}$ , and  $P_r \sim P_s \sim 0.5$ , we obtain the average mobility  $\mu_{\text{av}} \approx 2.6 \times 10^5 \text{ nm}/(\text{s pN})$ , while the correction factor in Eq. (4.8) is 0.998, i.e., very close to 1. Hence, this gives rise to the ratio

$$\frac{\mu}{\mu_M} \approx 13, \quad (4.9)$$

in comparison with the value estimated in Ref. [47]:

$$\mu_M = \frac{1}{\zeta_p}. \quad (4.10)$$

The origin of the discrepancy between the present result and that of Ref. [47] is the slight difference between the models. In the strained state Ref. [47] operates with two characteristic times, that of  $S \rightarrow R$  conversion, i.e., the residence time Eq. (3.20)  $\langle t \rangle_s = 1/g_r$ , and the time of the restoration of bonds between the motor working head and the groove, which is much smaller. In the present model the two times are assumed equal, corresponding to the assumption that the spring relaxation  $S \rightarrow R$  is initiated when the working head becomes attached to the groove again. From a physical point of view this is equally possible, but implies that the motor spends

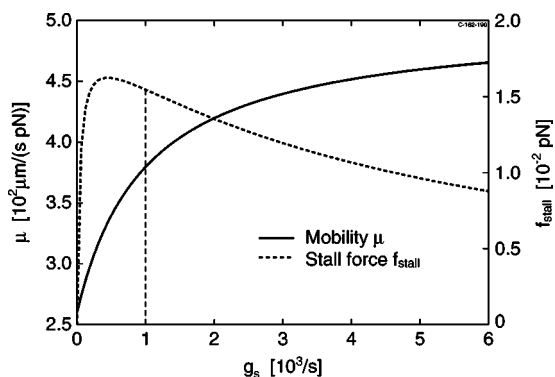


FIG. 4. Mobility  $\mu$  and stall force  $f_{\text{stall}}$  as a function of the hydrolysis rate  $g_s$ . The vertical line marks the value from Ref. [47]. Note the different scales.



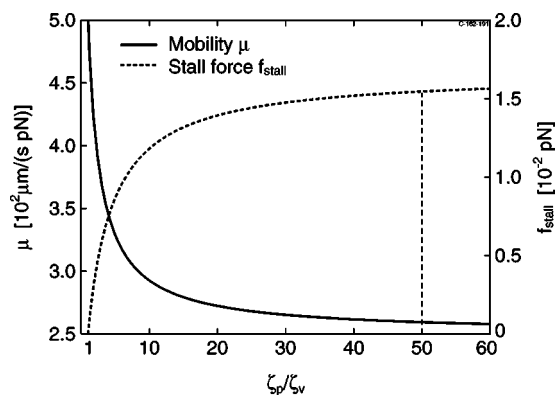


FIG. 5. Mobility  $\mu$  and stall force  $f_{\text{stall}}$  as a function of the protein friction  $\zeta_p$  (model value  $5.0 \times 10^{-5}$  nm/s pN).

much shorter times in state  $S$  than in state  $R$ , or  $g_r \gg g_s$ , i.e.,  $P_r \sim 1$  and  $P_s \sim 0$ , and the motor becomes much more volatile to the local force during these periods.

From the mobility  $\mu$  and the zero-load velocity  $\langle v_x^0 \rangle$ , we obtain the stall force

$$f_{\text{stall}} = \frac{\langle v_x^0 \rangle}{\mu}. \quad (4.11)$$

In Figs. 4 and 5 we have on the same plots depicted the values of the mobility  $\mu$  and the stall force  $f_{\text{stall}}$  versus the hydrolysis rate  $g_s$  and the protein friction  $\zeta_p$ . We note that the stall force exhibits a maximum as a function of  $g_s$  close to the parameter values chosen in our calculations, whereas the mobility is close to saturation. Similarly, as a function of  $\zeta_p$ , the stall force is close to its maximum value, whereas the mobility does not change much within the chosen plot range (note that the ordinate does not reach the origin). In general, we observe that due to the particular dependence of  $\mu$  on the model parameters, its value varies relatively weakly within large intervals for the individual parameter values. In Fig. 6 we have depicted the mobility and stall force as functions of the rate of relaxation  $g_r$ . For large  $g_r$  we obtain a stall force of the order of piconewtons, which is in the biological range.

## V. SUMMARY AND CONCLUSION

In this paper we have by analytical means solved a molecular motor model proposed by Mogilner *et al.* [47]. This model represents a robotic motor solely based on an effective static friction interaction between motor and its support (track). From the underlying Langevin equations, which represent the synchronized dichotomous processes of friction, effective spring constant, and distance between the motor heads, we obtain explicit expressions for the load-free motor velocity, the mobility of the motor, and the stall force. Whereas the result for the load-free velocity produces a typical motor velocity of several  $\mu\text{m/s}$  for physiologically reasonable parameters, the exact solution overestimates the mo-

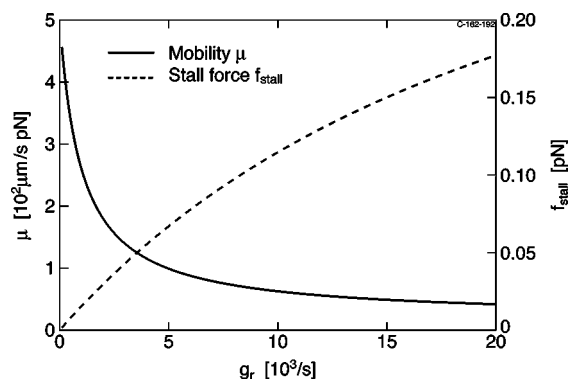


FIG. 6. Mobility  $\mu$  and stall force  $f_{\text{stall}}$  as a function of the rate of relaxation  $g_r$ . We observe that for large relaxation rate the stall force enters the biological range.

bility, leading to a value for the stall force that is roughly two orders of magnitude smaller than physiological values and significantly smaller than the simulation results reported in Ref. [47]. This variance is associated with a difference in the stochastic dynamics underlying the analysis and the dynamical processes implied in the numerical simulation.

A likely explanation relies on an essential feature of an model, which is the decoupling of the dynamics of the motor protein–rail biopolymer interaction (chemical bonds forming and breaking) into a fast, detached process during energy consumption, and a slow relaxing process in one mechanochemical motor cycle. This purely stochastic picture leads to situations in which the motor detaches frequently, before its relaxing step is finished, and therefore the subcycles, which actually lend themselves to propulsion, are interrupted. Obviously, this leads to the underestimation of the stall force. In a real system, the fact that chemical bonds are established ensures that a full propulsion subcycle can be completed before dissociation takes place for the next loading of the internal motor “spring” in parallel to hydrolysis. In comparison to the ratchet models in which the motor properties are represented by fluctuating between two different, periodic potentials, it appears that the latter rely on fewer parameters, and therefore their stall force can be adjusted better to actually observed values.

We finally should like to emphasize that the exact results obtained allow for an exact and detailed study of the dependence of the motor characteristics on the various parameters without invoking numerical simulations. Additional features, such as the low likelihood for detaching from the rail during the forward motion, could be incorporated into the model and still be solved explicitly, using the solution schemes developed here. We therefore believe that this study leads to a better understanding of molecular motor models.

## ACKNOWLEDGMENT

We should like to thank John Hertz for very constructive discussions.

- [1] J. Howard, *Nature (London)* **389**, 561 (1997).
- [2] B. Alberts, K. Roberts, D. Bray, J. Lewis, M. Raff, and J. D. Watson, *Molecular Biology of the Cell* (Garland, New York, 1994).
- [3] J. Howard, *Mechanics of Motor Proteins and the Cytoskeleton* (Sinauer Associates, Sunderland, MA, 2001).
- [4] P. Reimann, *Phys. Rep.* **361**, 57 (2002).
- [5] R. C. Woledge, N. A. Curtin, and E. Homsher, *Energetic Aspects of Muscle Contraction* (Academic, London, 1985).
- [6] L. Stryer, *Biochemistry* (Freeman, San Francisco, 1988).
- [7] J. Darnell, H. Lodish, and D. Baltimore, *Molecular Cell Biology* (Scientific American Books, New York, 1990).
- [8] R. H. Abeles, P. A. Frey, and W. P. Jencks, *Biochemistry* (Jones and Bartlett, New York, 1992).
- [9] S. Leibler, *Nature (London)* **370**, 412 (1994).
- [10] A. A. Simpson *et al.*, *Nature (London)* **408**, 745 (2000).
- [11] M. Badoual, F. Jülicher, and J. Prost, *Proc. Natl. Acad. Sci. U.S.A.* **99**, 6696 (2002).
- [12] K. Svoboda and S. M. Block, *Cell* **77**, 773 (1994).
- [13] K. Svoboda, P. P. Mitra, and S. M. Blockthor, *Proc. Natl. Acad. Sci. U.S.A.* **91**, 11782 (1994).
- [14] H. Kojima, E. Muto, H. Higuchi, and T. Yanagida, *Biophys. J.* **73**, 2012 (1997).
- [15] H. Higuchi, E. Muto, Y. Inoue, and T. Yanagida, *Proc. Natl. Acad. Sci. U.S.A.* **94**, 4395 (1997).
- [16] C. M. Coppin, D. W. Pierce, L. Hsu, and R. D. Vale, *Proc. Natl. Acad. Sci. U.S.A.* **94**, 8539 (1997).
- [17] M. D. Wang, M. J. Schnitzer, H. Yin, R. Landick, J. Gelles, and S. M. Block, *Science* **282**, 902 (1998).
- [18] A. D. Mehta, M. Rief, J. A. Spudich, D. A. Smith, and R. M. Simmons, *Science* **283**, 1689 (1999).
- [19] T. Strick, J.-F. Allemand, V. Croquette, and D. Bensimon, *Phys. Today* **54**(10), 46 (2001).
- [20] D. E. Smith, S. J. Tans, S. B. Smith, S. Grimes, D. L. Anderson, and C. Bustamante, *Nature (London)* **413**, 748 (2001).
- [21] M. E. Fisher and A. B. Kolomeisky, *Proc. Natl. Acad. Sci. U.S.A.* **96**, 6597 (1999).
- [22] S. Leibler and D. A. Huse, *J. Cell Biol.* **121**, 1357 (1993).
- [23] T. Duke and S. Leibler, *Biophys. J.* **71**, 1235 (1996).
- [24] M. Magnasco, *Phys. Rev. Lett.* **71**, 1477 (1993).
- [25] F. Jülicher, A. Ajdari, and J. Prost, *Rev. Mod. Phys.* **69**, 1269 (1997).
- [26] R. D. Astumian, *Science* **276**, 917 (1997).
- [27] R. D. Astumian and I. Derenyi, *Biophys. J.* **77**, 993 (1999).
- [28] R. D. Astumian and P. Hänggi, *Phys. Today* **55**(11), 33 (2002).
- [29] H. Ambaye and K. W. Kehr, *Physica A* **267**, 111 (1999).
- [30] A. Ajdari, D. Mukamel, L. Peliti, and J. Prost, *J. Phys. I* **4**, 1551 (1994).
- [31] B. Norden, Y. Zolotaryuk, P. L. Christiansen, and A. V. Zolotaryuk, *Appl. Phys. Lett.* **80**, 2601 (2002).
- [32] A. Vilfan, E. Frey, and F. Schwabl, *Eur. Phys. J. B* **3**, 535 (1998).
- [33] A. Vilfan and T. Duke, *Biophys. J.* **85**, 818 (2003).
- [34] H. Y. Lee and M. Kardar, *Phys. Rev. E* **64**, 056113 (2001).
- [35] D. P. Mulvihill and J. S. Hyams, *Nat. Cell Biol.* **3**, E1 (2001).
- [36] R. J. Pelham and F. Chang, *Nature (London)* **419**, 82 (2002).
- [37] M. von Smoluchowski, *Phys. Z.* **13**, 1069 (1912).
- [38] R. P. Feynman, R. B. Leighton, and M. Sands, *The Feynman Lectures on Physics* (Addison-Wesley, Reading, MA, 1963).
- [39] A. F. Huxley, *Prog. Biophys. Biophys. Chem.* **7**, 255 (1957).
- [40] C. Kettner, P. Reimann, P. Hänggi, and F. Müller, *Phys. Rev. E* **61**, 312 (2000).
- [41] S. Matthias and F. Müller, *Nature (London)* **424**, 53 (2003).
- [42] A. K. Vidybida and A. A. Serikov, *Phys. Lett.* **108A**, 170 (1985).
- [43] K. Tawada and K. Sekimoto, *J. Theor. Biol.* **150**, 193 (1991).
- [44] G. Jannink, B. Duplantier, and J. L. Sikorav, *Biophys. J.* **71**, 451 (1996).
- [45] C. J. Brokaw, *Biophys. J.* **73**, 938 (1997).
- [46] Y. Imafuku, Y. Y. Toyoshima, and K. Tawada, *Biophys. J.* **70**, 878 (1996).
- [47] A. Mogilner, M. Mangel, and R. J. Baskin, *Phys. Lett. A* **237**, 297 (1998).
- [48] K. Kaseda, H. Higuchi, and K. Hirose, *Nat. Cell Biol.* **5**, 1079 (2003).